Metadata of the chapter that will be visualized online

Chapter Title	A Tutorial Review on Sporadic *E* Layers	
Chapter Sub-Title		
Chapter CopyRight - Year	Springer Science+Business Media B.V. 2011 (This will be the copyright line in the final PDF)	
Book Name	Aeronomy of the Earth's Atmosphere and Ionosphere	
Corresponding Author	Family Name	**Haldoupis**
	Particle	
	Given Name	**Christos**
	Suffix	
	Division	Physics Department
	Organization	University of Crete
	Address	Heraklion, Crete, Greece
	Email	chald@physics.uoc.gr

Abstract

The sporadic *E* layers (*Es*) form in the dynamo region of the ionosphere when metallic ions of meteoric origin are converged vertically in a wind shear. This paper provides a comprehensive update on sporadic *E,* a topic that has been studied for many years. The aim is to render useful information and physical understanding for both the general and specialized reader, and construct an integrated picture of sporadic *E* through a critical synthesis of recent findings. The basic aspects of the layer windshear theory are reviewed and then selected observations are presented which are tested against the theoretical predictions. The emphasis is placed on the tidal wind control of the diurnal and semidiurnal variability and altitude descent of sporadic *E* layers. There is now enough evidence to suggest that mid- and low-latitude sporadic *E* is not as "sporadic" as the name implies but a regularly occurring ionospheric phenomenon. This suggests that *E* layer physics could also be incorporated in existing atmosphere-ionosphere coupling models. Furthermore, the present review summarizes recent findings which provide physical insight into long-going problems and questions about the seasonal dependence and the global occurrence of *Es*. The experimental results, which are in favor of the windshear theory, imply that the key agents controlling sporadic E are: tidal wind atmospheric dynamics, the Earth's horizontal magnetic field component, and the meteoric deposition of metallic material in the lower thermosphere.

Chapter 29

A Tutorial Review on Sporadic *E* Layers

Christos Haldoupis

Abstract The sporadic *E* layers (*Es*) form in the dynamo region of the ionosphere when metallic ions of meteoric origin are converged vertically in a wind shear. This paper provides a comprehensive update on sporadic *E,* a topic that has been studied for many years. The aim is to render useful information and physical understanding for both the general and specialized reader, and construct an integrated picture of sporadic *E* through a critical synthesis of recent findings. The basic aspects of the layer windshear theory are reviewed and then selected observations are presented which are tested against the theoretical predictions. The emphasis is placed on the tidal wind control of the diurnal and semidiurnal variability and altitude descent of sporadic *E* layers. There is now enough evidence to suggest that mid- and low-latitude sporadic *E* is not as "sporadic" as the name implies but a regularly occurring ionospheric phenomenon. This suggests that *E* layer physics could also be incorporated in existing atmosphere-ionosphere coupling models. Furthermore, the present review summarizes recent findings which provide physical insight into long-going problems and questions about the seasonal dependence and the global occurrence of *Es*. The experimental results, which are in favor of the windshear theory, imply that the key agents controlling sporadic E are: tidal wind atmospheric dynamics, the Earth's horizontal magnetic field component, and the meteoric deposition of metallic material in the lower thermosphere.

C. Haldoupis (✉)
Physics Department, University of Crete, Heraklion, Crete, Greece
e-mail: chald@physics.uoc.gr

29.1 Introduction

The name "sporadic *E*" and its abbreviation "*Es*" refer to a legendary ionospheric phenomenon which is known since the recording of the first primitive ionograms in the early nineteen thirties. It is a generic term used for the thin layers of enhanced metallic ionization that form in the *E* region ionosphere, mostly between about 95 and 120 km. These can at times become denser than the normal *E* layer or even the peak *F* layer, thus they may affect HF radio propagation and *F* region ionosonde recordings severely and therefore can be of relevance to space weather.

Sporadic *E* has been investigated extensively, both experimentally and theoretically. Albeit the great majority of the observational studies have been performed with ionosondes, there are also a considerable number of investigations carried out with incoherent and coherent scatter radars as well as through probing in-situ with rockets. It is not the purpose of this paper to critically summarize all these numerous results and the interested reader should consult past review papers by Whitehead (1989) and Mathews (1998) and the references cited therein, as well as more recent publications quoted in the present paper.

The scope here is to provide a tutorial review on Sporadic *E* that summarizes our present understanding. Instead of providing a detailed treatise of the phenomenon and its complexities, we focus here on basic physical principles and key observational characteristics. An objective is to emphasize a fact that has been overlooked, that is, sporadic *E* is not as "sporadic" as its name implies but rather a regularly occurring phenomenon over a large range of latitudes from a few degrees off the magnetic equator to the auroral zones.

M.A. Abdu, D. Pancheva (eds.), A. Bhattacharyya (Coed.), *Aeronomy of the Earth's Atmosphere and Ionosphere*, IAGA Special Sopron Book Series 2, DOI 10.1007/978-94-007-0326-1_29,

In the following, key theoretical elements which form the basis of sporadic E understanding are presented, followed by the presentation and discussion of selected experimental properties.

29.2 Basic *Es* Theory and Processes

Here, basics of the midlatitude sporadic E theory are presented, which are pertinent to the scope of the present paper and useful in obtaining a clear physical understanding. The physics of sporadic E layer formation is described through the *Windshear Theory*, first proposed and formulated in the early sixties by Whitehead (1961), and Axford (1963), and since developed further by more authors (e.g., see Whitehead, 1989). It relies on the idea that thin layers of ionization can form in the dynamo region of the ionosphere by vertical ion convergence driven by vertical shears in the horizontal neutral wind.

This layer-forming process is controlled fully by ion dynamics, which can be adequately expressed through a simplified version of the ion momentum equation. Following Chimonas and Axford (1968) and neglecting pressure gradient (diffusion) forces at E region heights, gravity, as well as electric field forces at middle and low latitudes, the equation of ion motion includes at steady state only the ion-neutral collisional and geomagnetic Lorentz forces:

$$m_i\, \nu_i(\mathbf{v}_i - \mathbf{U}_n) - e\,\mathbf{v}_i \times \mathbf{B} = 0, \tag{29.1}$$

where m_i and ν_i are the ion mass and ion-neutral collision frequency, $\mathbf{v}_i$ and $\mathbf{U}_n$ are the ion drift and neutral wind velocities respectively, e is the electronic charge, and $\mathbf{B}$ the geomagnetic field vector. By adopting a geomagnetic south, geomagnetic east and vertically up Cartesian (x,y,z) coordinate system for the northern hemisphere, and using the notations of Mathews (1998) for the vectors $\mathbf{v}_i$ (u, v, w), $\mathbf{U}_n$ (U, V, W) and $\mathbf{B}$ ($-B\cos I$, 0, $-B\sin I$), Eq. (29.1) can be solved for the (positive upwards) vertical ion drift:

$$w = \frac{(\nu_i/\omega_i)\cos I}{1+(\nu_i/\omega_i)^2}V + \frac{\cos I \sin I}{1+(\nu_i/\omega_i)^2}U = f_{zn}\,V + f_{mr}\,U. \tag{29.2}$$

Here, I denotes the magnetic dip angle while ν_i/ω_i is the ratio of ion-neutral collision frequency to ion gyrofrequency, which introduces an altitude dependence through the decrease with altitude of the ion-neutral collision frequency. The dimensionless parameters f_{zn} and f_{mr} represent the zonal and meridional "ion drift factors". In deriving Eq. (29.2), it is assumed that the vertical wind component is negligible, that is, $W \approx 0$, an assumption that is fairly reasonable.

29.2.1 *Windshear Ion Convergence Mechanisms*

The first and second terms in the right hand side of Eq. (29.2) define two processes of vertical ion convergence which associate with the vertical shears in zonal (V) and meridional wind (U), respectively. The zonal wind shear mechanism is illustrated in the upper part of Fig. 29.1. It involves the horizontal component of the magnetic field $B_H = B\cos I$ and a vertical wind shear characterized by a westward wind above and an eastward wind below. As the ions drift with the wind to the west above (east below) with V_{west} (V_{east}) they are also Lorentz-forced $eV_{\mathrm{west}}B_H$ ($eV_{\mathrm{east}}B_H$) to drift downwards (upwards), therefore converging at an angle to the wind shear null, where $V = 0$, to accumulate and form a layer. The lower part of Fig. 29.1 sketches the meridional wind shear mechanism which requires (for the northern hemisphere) a northward wind above and a southward wind below. Here, the ions are wind-driven horizontally while at the same time they are constrained by the Lorentz force to gyrate about the inclined magnetic field lines. As a result, the ions finally move in the direction of the magnetic field with the wind velocity component $U_{\mathrm{north}}\cos I$ ($U_{\mathrm{south}}\cos I$) and therefore converge to the wind shear null at $U = 0$ to form a layer. Since the electrons are strongly magnetized ($\omega_e >> \nu_e$), they are not affected directly by neutral winds. Therefore, in the ion convergence processes under discussion, the electrons are Coulomb-forced to follow the ions, moving along the magnetic field lines to maintain plasma neutrality.

Note that none of the two ion-convergence mechanisms will work well near the magnetic equator where the magnetic field is fairly horizontal. In the case of a meridional wind shear, the wind simply moves the ions along the field lines thus the Lorentz force is zero and the ions do not move vertically. In the zonal wind

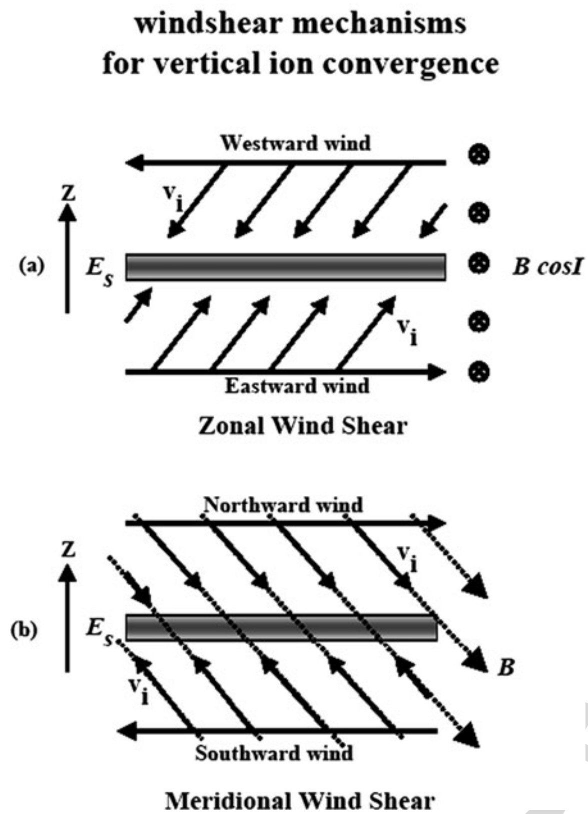

Fig. 29.1 Exemplifying sketches of the zonal (*top*) and meridional (*bottom*) wind shear mechanisms for vertical ion-convergence into a thin ionization layer forming at the wind shear velocity null. More details on the two mechanisms are given in the text

shear process the ions are strongly Lorentz-forced to move vertically, however they cannot converge into a layer easily because they are kept near a fixed magnetic field line by the strongly magnetized electrons, because the plasma must remain neutral. Also, both windshear mechanisms do not work efficiently at high magnetic latitudes (auroral zones). There, the horizontal magnetic field component which is involved in the zonal windshear process is small, whereas for the meridional windshear process the driving wind component along the magnetic field is also small. As a result of the aforementioned geometrical constraints, the strongest and more frequent layers occur at midlatitudes. We note however that the sporadic *E* layers seen occasionally at high latitudes are attributed mostly to the relatively large auroral electric fields which in this case do enter also in Eq. (29.1).

Es layers live long times (from a few to many hours), implying that the windshear ion convergence process cannot rely on ambient molecular ions which live short times, because they neutralize quickly (in a few minutes) through dissociative recombination. To get around this problem, it was suggested that *Es* layers are due to metallic (monoatomic) ions of meteoric origin undergoing slow radiative recombination which requires a three body collision. This fact has been confirmed by rocket and incoherent scatter radar observations (e.g. see Whitehead, 1989 and Mathews, 1998). Note that the metallic ion lifetimes range widely with altitude, from a few days at ∼120 km to a few hours at ∼95 km (MacDougall et al., 2000).

29.2.2 Ion-Convergence Times

The layer-forming efficiency of the zonal and meridional windshear mechanisms at a given altitude differ because their ion drift factor dependence on ν_i/ω_i is different. This is illustrated in Fig. 29.2, which presents the zonal and meridional ion drift factors for a typical midlatitude location as a function of altitude. The ν_i/ω_i

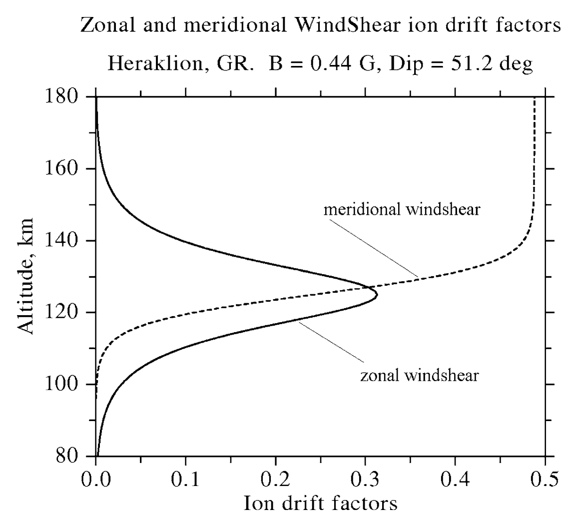

Fig. 29.2 Altitude variation of the zonal and meridional windshear ion drift factors (see Eq. (29.2)) for a typical midlatitude location. They determine the mechanisms' layer forming efficiency at different altitudes. The zonal windshear ion-convergence dominates below 115 km, at altitudes where the majority of sporadic *E* layers are situated

altitude profile used here was taken from Bishop and Earle (2003) and refers to metallic ion plasma with a mean ionic mass 40 AMU. As seen, both mechanisms are equally effective at around 125 km where $\nu_i \sim \omega_i$, while at lower (upper) altitudes the zonal (meridional) windshear mechanism becomes dominant. At upper heights the ion-neutral collision frequency is reduced which makes the ions more magnetized, therefore the ability of a zonal wind to move them across the magnetic field is weakened. On the other hand, the meridional windshear process, which moves the ions along the inclined magnetic field direction, works better if the ions are strongly magnetized therefore it dominates at upper heights where $\omega_i \gg \nu_i$.

At lower *E* region heights where collisions are more frequent, the ions become less magnetized, which reduces the action of Lorentz force. This affects both windshear mechanisms but the effect is more severe in the meridional rather than the zonal windshear process. Figure 29.2 shows that the meridional windshear effects on ion vertical motion become minimal below ~115 km, thus ion convergence and *Es* layer forming at altitudes below 115 km is governed by the vertical shears in the zonal wind. The latter can still affect the layers down to altitudes 90 and even 85 km, as suggested by incoherent scatter radar observations of weak lower altitude *Es*.

Equation (29.2) can be used to estimate the time required for ion convergence to cover a vertical distance Δz, as a function of altitude (through the ion-neutral collision frequency) and neutral wind velocity for both the zonal and meridional wind shear mechanisms:

$$t_{zn} = \frac{1 + (\nu_i/\omega_i)^2}{V(\nu_i/\omega_i)\cos I}\Delta z \quad \text{and} \quad t_{mr} = \frac{1 + (\nu_i/\omega_i)^2}{U \cos I \sin I}\Delta z. \tag{29.3}$$

Such estimates are useful in understanding the layer altitude descent with time, as it will be discussed later. Figure 29.3 shows estimates of vertical ion convergence times for the same midlatitude location and the ion-neutral collision frequency profile used in Fig. 29.2. The ion convergence times were computed for $\Delta z = 1$ km, separately for a strong (weak) zonal and meridional wind components of 100 m/s (10 m/s). As one may infer, a typical meridional wind of 50 m/s can force the ions to drift 1.0 km vertically in a few minutes at altitudes above 120 km, whereas below

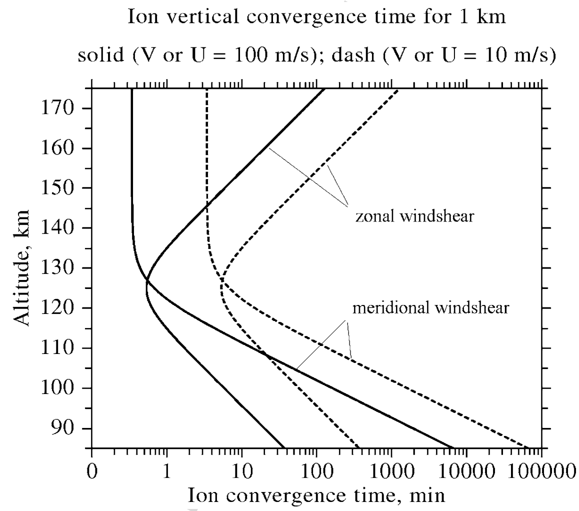

Fig. 29.3 Ion-convergence time estimates as a function of altitude for the zonal and meridional wind shear mechanisms, computed for strong (*solid*) and weak (*dash*) wind driving conditions. See text for details

100 km this requires times of the order of hours. On the other hand, a zonal wind is much more efficient in forcing the ions to move vertically faster at lower altitudes compared to an equally strong meridional wind there. For example, at 110 km the ions need ~10 min to move one kilometer vertically under the forcing of a 50 m/s zonal wind, but ~100 min for a meridional wind of the same magnitude.

It is important to realize that vertical ion-convergence becomes vertical ion-divergence for a windshear polarity opposite of that forming a layer. In this way an existing layer can be broadened and possibly be dissolved by a vertical windshear acting to move the ions apart, for instance in the case of a wind shear in which the wind is eastward above and westward below. Expectedly, the times required for windshear *de-layering* are about the same as for layer forming, which means that the layers can de-form faster (slower) at the altitudes where they form faster (slower). This is the reason why *Es* layers remain fairly stable for many hours at lower heights, especially below 100 km where ion-convergence, or divergence, times are long. On the other hand, at upper heights near 125 to 130 km, layers are more variable and shorter-lived since ion-convergence (divergence) is much faster there.

29.2.3 Plasma Diffusion

A process that acts against ion convergence is ambipolar plasma diffusion. Diffusion is commonly ignored in the sporadic *E* forming process because the ambipolar diffusion coefficient $D_a = k_B(T_i + T_e)/m_i\nu_i$ is small at *E* region altitudes. The role of plasma diffusion becomes increasingly important at upper *E* region altitudes where D_a increases because ion-neutral collisions decrease (e.g., D_a is ~1200 m^2/s at 150 km as compared to ~50 m^2/s at 100 km). Ambipolar plasma diffusion is the physical reason why sporadic *E* layers appear to be wider at higher E region altitudes, despite that meridional wind shear convergence there is more effective in layer formation (e.g., see Fig. 29.3). This also explains why strong wind shears in the *F* region meridional wind cannot form there narrow layers.

To estimate the importance of plasma diffusion in the layering process, we follow Axford (1963) and Kelley (1989) and take a sinusoidal form for a tidal zonal $V = V_0 \sin(k_z z)$, or meridional $U = U_0 \sin(k_z z)$, wind profile where V_0, U_0 and k_z $(=2\pi/\lambda_z)$ are the characteristic wind speed amplitudes and the vertical tidal wavenumber, respectively. Then, plasma diffusion prevents a layer from forming when the characteristic diffusion time $\tau_D = 1/(k_z^2 D_a)$ is smaller than the typical zonal (meridional) windshear plasma convergence time taken from Eq. (29.3), that is:

$$\tau_D \le \frac{1 + (\nu_i/\omega_i)^2}{k_z V_0 (\nu_i/\omega_i)\sin I}; \quad \tau_D \le \frac{1 + (\nu_i/\omega_i)^2}{k_z U_0 \cos I \sin I}. \tag{29.4}$$

Figure 29.4 exemplifies the zonal and meridional wind ion convergence and plasma diffusion times computed as a function of altitude for the same parameters used in the previous figures, and for wind speed amplitudes $V_0 = U_0 = 25$ m/s and a tidal vertical wavelength of $\lambda_z = 33$ km, which corresponds to the semidiurnal S(2,6) tidal mode. In this case, plasma diffusion is effective in opposing layer forming above ~140 km and ~180 km for the zonal and meridional windshear processes, respectively. On the other hand, diffusion times are fairly large at lower altitudes relative to convergence times there; therefore, correctly, plasma diffusion becomes unimportant in layer forming at lower heights, say below 130 to 120 km, where narrow sporadic *E* layers are mostly located.

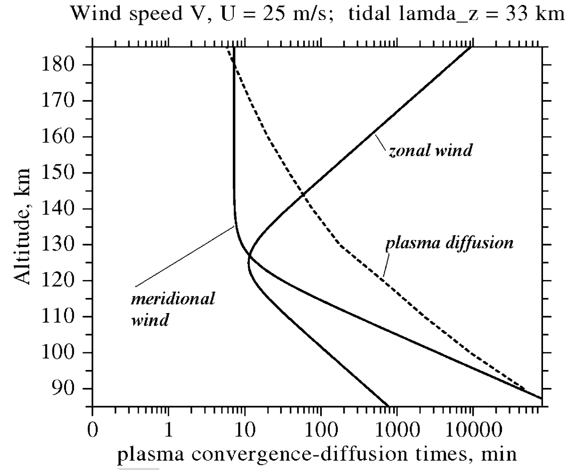

Fig. 29.4 Examples of vertical ion-convergence (or layer-forming) time estimates at different altitudes for a zonal and meridional wind (*solid lines*), as compared to plasma diffusion times (*dashed line*) estimated for a semidiurnal tidal wind of vertical wavelength $\lambda_z = 33$ km. Plasma diffusion has little effect in *Es* layer forming below about 130 km. See text for more details

29.3 *Es* Observational Properties and Interpretations

Here, selected observations that characterize key properties of sporadic E layers are presented. The emphasis is placed on incoherent scatter radar measurements, which show *Es* to be largely a non-sporadic phenomenon. The processes contributing to short-term *Es* variability, and thus to the layer sporadic character, are discussed only in brief. Recent developments on two important *Es* properties, that is, the pronounced seasonal dependence and the global distribution of sporadic *E* layer occurrence are also summarized. The results included here are interpreted in the framework of the windshear theory predictions.

29.3.1 The Non-sporadic Nature of Sporadic E

The windshear theory suggests that sporadic *E* is closely linked to atmospheric dynamics because its formation requires the presence of sheared winds in the lower thermosphere. Inherently, this implies that *Es* possesses a variable but regular character that reflects both, the complexity and repeatability of atmospheric wind and waves dynamics in the MLT (mesosphere – lower thermosphere) region. This has been confirmed by incoherent scatter radar (ISR) studies at Arecibo (Geog. Lat. $\sim$18° N; Magnetic dip $\sim$50°). Besides its advantage in measuring electron density profiles accurately with good time and altitude resolution, it is the superb sensitivity of $\sim$500 electrons per cm^3 of the Arecibo ISR which reveals that sporadic *E* is present nearly all times, that is, it exhibits a non-sporadic behavior, in general. The Arecibo ISR studies showed that there is a well defined tidal variability in sporadic *E*, which prompted Mathews (1998) to introduce the term "tidal ion layers" (TIL) as more appropriate to "sporadic *Es* ".

As discussed by Mathews (1998), the Arecibo ISR observations revealed that the diurnal and semidiurnal tides are the main agents that control the formation and altitude descent of sporadic E layers. This was recognized to be also true at higher midlatitudes by Haldoupis et al. (2006) who used a novel method to identify tidal variations and altitude descent in ionogram data. On the average, the tidal winds may dominate and thus govern the diurnal and sub-diurnal variability and descent of the layers through their vertical wind shears which form and drag the layers along as they phase speed propagate downwards. The close connection between *Es* and tides is to be anticipated because, as shown for example by Chapman and Lindzen (1970) and Forbes et al. (2007), the neutral winds in the E region are dominated by solar tides. This setup agrees fairly well with windshear theory, which, as discussed previously, favors metallic ion layer formation at vertical shear convergence nulls. However, atmospheric dynamics in the E region can occasionally become rather complex, which may lead to departures from the predominant tidal wind pattern (Larsen, 2002).

The term "sporadic" had been labeled at times as "convenient" and "improper" well before the Arecibo ISR observations. This happened because it was realized that this term was adopted to a large extent as a result of an instrumental limitation rather than of a prominent physical property. The limitation, which made a variable ionospheric phenomenon appear more sporadic in occurrence than it actually is, relates with the fact that the ionosonde electron density measurements are inevitably subject to a sharp lower cutoff near 2.5×10^4 cm^{-3} caused by the instrument's lowest transmitted frequency of $\sim$1.0 to 1.5 MHz. Thus, whenever the peak electron density in a layer would decrease below (increase above) the minimum electron density detected by ionosonde, the layer would disappear (appear), therefore making its occurrence to appear sporadic.

Figures 29.5 and 29.6 show Arecibo ISR observations, presented here in order for the reader to appreciate that *Es* follows a predictably repeating pattern,

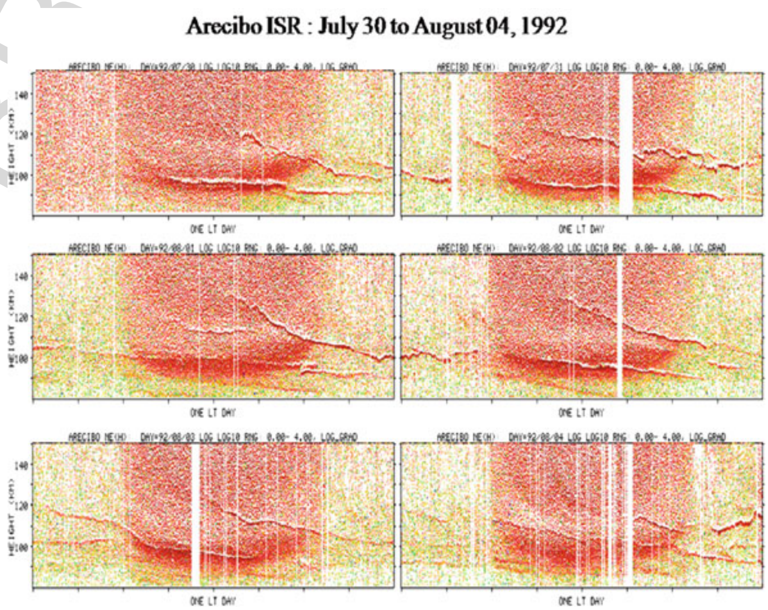

Fig. 29.5 Arecibo incoherent scatter radar *log(dNe/dz)* height-time-intensity plots measured for six consecutive days, showing a regular and repeating pattern of sporadic *E* layer occurrence. This is characterized by lower and upper *E* region altitude layers, which descend in altitude during the course of the day. The lower altitude layers appear to follow a well-defined diurnal variation which is apparently controlled by the diurnal tide

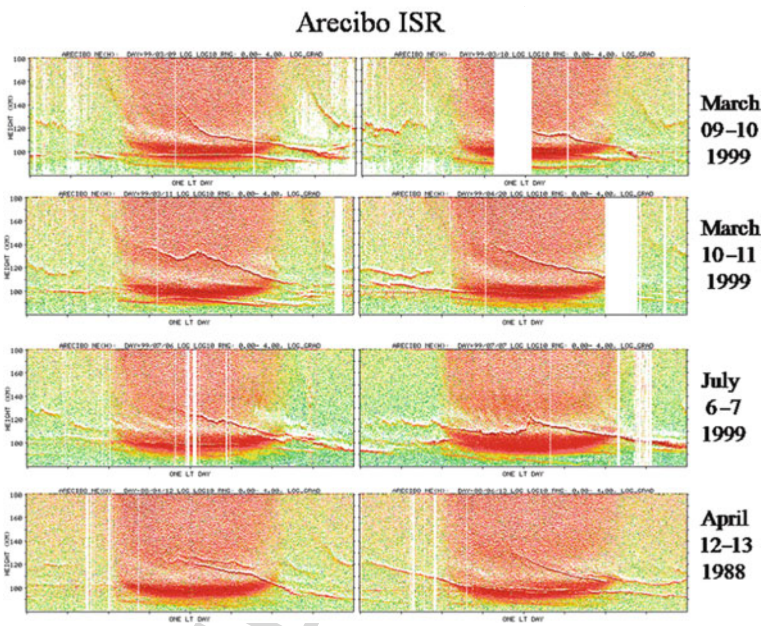

Fig. 29.6 Same as Fig. 29.5. It presents Arecibo ISR observations of daily sporadic *E* trace activity, which shows a repeating pattern of diurnal and semidiurnal periodicities in layer formation and altitude descent controlled by the diurnal and semidiurnal tides

determined by the tidal modes in the lower thermosphere. Figure 29.5 illustrates a prevailing *Es* tidal variability both in time and altitude, observed during 6 full days of continuous Arecibo ISR operation. Each panel corresponds to a 24-h local day and represents a height-time-intensity (HTI) plot, where the "intensity" here refers to the logarithm of the (positive) vertical electron density gradient, *log(dNe/dz)*. This type of display is quite useful for detecting the altitude location of *Es* layers quite accurately during the course of a 24-h local day, and thus is suitable in identifying the tidal variability and descent of layers with time. As seen in Fig. 29.5, there is a daily trace pattern that exhibits iterating characteristics dominated by tidal-like periodicities. Figure 29.6 presents more typical Arecibo observations obtained from various radar runs, each lasting at least two 24-h days. Shown there are height-time-*log(dNe/dz)* intensity 24-h local day plots which illustrate a repeating pattern in sporadic layer formation and descent.

Inspection of the HTI plots, in both Figs. 29.5 and 29.6, shows that for a given 24-h local day there is usually a set of 3 different *Es* traces. These include a diurnal trace at lower altitudes below about 110 km and two semidiurnal-like upper altitude traces, a daytime trace and a less frequent nighttime trace, which appear at about 140 km prior to noon and midnight, respectively. The lower altitude diurnal layer trace is descending with a speed ∼1.0 km/h which agrees reasonably well with the phase velocity of the theoretical diurnal tidal mode S(1,1) which has a vertical wavelength of ∼28 km and is known to be dominant below 110 km at lower midlatitudes (e.g., see Harper, 1977). The upper altitude semidiurnal-like layers descend with speeds of about 2–4 km/h towards lower heights to often merge there with the slowly descending diurnal layer below. This repeating *Es* trace pattern shows that sporadic *E* exhibits a well-defined regularity in both formation and altitude descent, in response to tidal windshear dynamics.

As mentioned, Figs. 29.5 and 29.6 show a noticeable difference between the upper altitude semidiurnal layers. That is, the nighttime layer is often much weaker and less frequent than the daytime one. This is likely because the tidal windshear associated with the formation of the daytime semidiurnal layer collects the metallic ion population produced by the enhanced meteoric influx during past-midnight to morning hours and the subsequent photoionization of metallic atom deposition. In this way, the medium is depleted of metallic ions later in the day, which implies that it may become difficult for the upper nighttime layer to reach always detectable levels.

The seasonal tidal variability and descent of *Es* layers at Arecibo were studied statistically by Christakis et al. (2009), using for analysis a large ISR data set

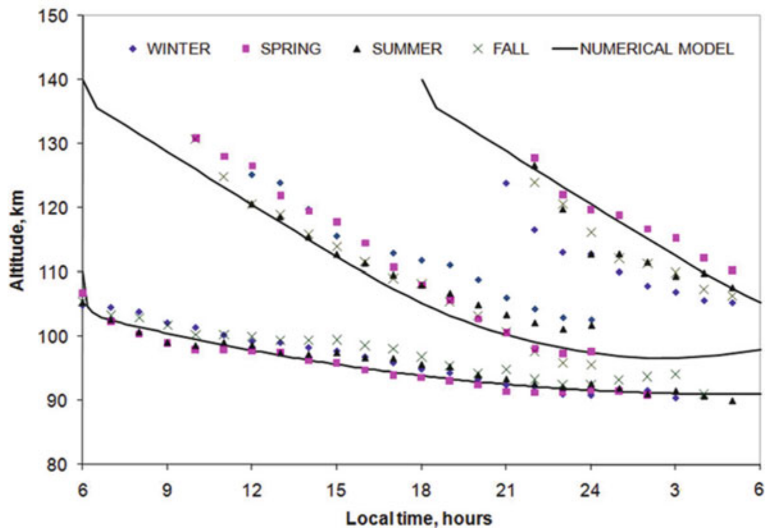

Fig. 29.7 The three sets of points represent seasonal averages for the low altitude diurnal and the upper altitude semidiurnal sporadic *E* layer daily traces as observed by the incoherent scatter radar at Arecibo. The superimposed lines are windshear theory numerical simulations for a diurnal S(1,1) tidal wind mode with a vertical wavelength $\lambda_z = 28$ km (*lower altitude line*) and a semidiurnal S(2,6) zonal tidal wind with $\lambda_z = 33$ km (*upper altitude lines*)

of 140 days of radar operation, distributed over several years and covering evenly all seasons. The key findings are summarized in Fig. 29.7, which shows the hourly mean altitude positions of the prevailing diurnal and semidiurnal *Es* layers. As seen, there is a three layer daily pattern prevailing, with some differences, in all seasons. The solid lines superimposed on top of the three sets of mean seasonal *Es* trace points represent numerical simulations computed form windshear theory (by solving Eq. (29.2)), using a simplified diurnal or semidiurnal zonal tidal wind of a given amplitude and vertical wavelength λ_z. It was found that the S(1,1) 24-h tide with a vertical wavelength $\lambda_z \sim 25$ km controls fully the formation and descent of metallic *Es* layers at low altitudes below ~110 km. The higher altitude layers and their altitude descent was approximately accounted for by using the semidiurnal tidal mode S(2,6) with $\lambda_z \sim 35$ km.

29.3.2 Physical Interpretation

Taking into consideration the observations and theoretical predictions discussed previously, a physical picture emerges which is summarized as follows. First, let's take the upper altitude daytime and nighttime descending layers that are controlled by a semidiurnal tide. These are associated with the so called intermediate descending layers which often detach from the *F* region bottomside (Mathews, 1998). They form at shear convergence nulls at higher *E* region altitudes (say, 150–180 km) but they become narrow only below about 135 km because plasma diffusion, which counteracts ion-convergence and plasma accumulation, becomes now ineffective below ~140 km (see Fig. 29.4).

According to the windshear theory, a layer remains in a shear convergence null only if it forms fast enough compared to the time required for the null to phase-propagate downward a distance equal to the layer's width. In the upper *E* region the layers form rapidly (see Fig. 29.3) thus they tend to "stick" at a wind shear convergence null as it moves downwards with the vertical tidal phase speed. This is manifested by the steady negative slopes seen in *Es* traces above about 115 to 120 km (see Figs. 29.5 and 29.6), while below these heights the situation changes gradually because ion-neutral collisions become increasingly effective in opposing/delaying ion convergence. As a result, layer descent slows down (trace slopes in Fig. 29.5 start curving) because ion convergence time becomes increasingly larger (see Fig. 29.3), therefore a layer cannot form fast enough to remain inside a tidal convergence null as it does at upper *E* region heights. In fact, the layers lag steadily behind the downward propagating tidal convergence null, therefore they keep descending at rates progressively smaller than the vertical tidal phase velocity. This slow descent continues till a divergent tidal node that follows ion convergence catches up with *Es* to impose a possible de-layering effect because the layered ions tend now to disperse vertically. Depending upon the amplitude and phase velocity of the semidiurnal tide, there is finally a lower altitude near 110 km at which the ion neutral collision frequency is high enough to not allow the 12-h tide to affect the layer. At these altitudes and below, the semidiurnal tides and their associated ion convergent (or divergent) wind shears propagate through a stagnating layer without impacting on it.

The upper altitude semidiurnal tidal layers may merge with lower altitude metallic ionization to contribute in the formation of the prominent 24-h sporadic *E* layer that is controlled by the diurnal S(1,1) tide. Relative to the semidiurnal tides, the S(1,1) 24-h tide has larger amplitudes (e.g., see Harper, 1977) and a shorter vertical wavelength so that it phase-propagates downwards slower than the 12-h tides, therefore it provides the time needed to fully control *Es* layer formation and descent from about 110 km down to 90 km (see Figs. 29.5 and 29.6). Although, the *Es* picture can at a given day become more complicated (see such days in Figs. 29.5 and 29.6), because of the complexity of atmospheric dynamics and the confluence of coexisting tidal modes, as well as gravity wave and possible neutral wind instability effects, the overall pattern of sporadic *E* formation and descent remains fairly well defined and predictable.

29.3.3 Non-tidal Es Variability

Close inspection of the daily plots in Figs. 29.5 and 29.6, show that *Es* traces undergo at times a shorter term variability, which appears to be more prominent during nighttime, as manifested by trace (layer) multiplicity, disruptions and altitudinal distortions, all constituting departures from a clear diurnal/semidiurnal picture. This is because of various causes and physical processes which also enter into action to affect in a rather unpredicted way the *Es* layers, contributing therefore to a “sporadic” character of the phenomenon. One key reason for this is the complexity of atmospheric wave dynamics due to non-linear interactions that result to additional tidal modes. For example, Arecibo ISR (e.g. see Mathews, 1998) and ionosonde studies (e.g., see Haldoupis and Pancheva, 2006) revealed at times also a role for shorter period tidal modes, such as the quarterdiurnal and terdiurnal tides, on *Es* formation and descent. Naturally, it is the confluence of co-existing tidal modes, having different amplitudes and phases, which may create at times significant discrepancies from the dominant and regular diurnal and semidiurnal *Es* pattern.

Ionosonde studies over the last 10 years established that, in addition to the tides, planetary waves (PW) also play a role on *Es* generation which imposes long-term PW periodicities in the occurrence and intensity of sporadic *E* layers (e.g., see Haldoupis and Pancheva, 2002 and more references therein). Further studies, which involved careful analysis of simultaneous ionosonde and MLT neutral wind measurements, showed that the effect of PW on *Es* is impacted indirectly rather than directly. This seems to be done through the diurnal and semidiurnal tides which are modulated by planetary waves, apparently through a nonlinear interaction process at altitudes below 100 km (for details, see Pancheva et al., 2003 and Haldoupis et al., 2003).

At shorter scales, there exist a spectrum of gravity waves in the lower thermosphere which are also expected at times to have modulating effects on *Es* occurrence and intensity. Djuth et al. (2004) showed that gravity wave-like perturbations are imbedded in thermospheric electron density, and that “sets” of waves separated by 20–60 min can be present propagating rapidly downwards with speeds higher than say 100 km/h. These short period, large vertical wavelength gravity waves are weak ($\sim$1–3%) and require special data filtering methods in order to be identified, thus very rarely are visible in the type of displays shown in Figs. 29.5 and 29.6. A rare example of such a gravity wave set was observed during daytime before local noon in July 7, 1999, but their layering effect was weak and thus hardly visible in Fig. 29.5. Traces of such waves show up more easily in the upper *E* region plasma (see Djuth et al., 2004) and have a negative slope due to downward phase propagation which curves the traces towards increasing time as the phase front approaches lower *E* region heights where ion-neutral collisions become much more frequent. The wind shears associated with such waves can affect at times upper altitude sporadic *E* layers (e.g., see Mathews, 1998). Their effect is small below about 115 km apparently because the waves propagate fast through a layer, thus there is no time for their wind shears to impact much of vertical ion convergence or divergence effects on it.

Finally, there are also other forms of complex variability in sporadic *E* which are attributed to neutral air density and/or plasma instabilities as well as localized electrodynamic processes. Neutral instability mechanisms include the wind shear or Kelvin-Helmholtz and/or neutral convective instabilities which are responsible for short scale overturning structures such a Kelvin-Helmholtz billows characterized by vertical scales of a few kilometers and times scales of a hours (e.g., see Larsen, 2000; Larsen et al., 2004). Also plasma instabilities, like the two-stream and gradient-drift instabilities (e.g., see Hysell et al., 2002) can lead to the generation of medium to short scale electrostatic plasma irregularities which are field aligned and can cause strong backscatter of radar signals incident perpendicular to the earth's magnetic field. This is an important topic of sporadic *Es* plasma physics and electrodynamics that relates to the turbulent or unstable state of *Es* plasma, which, however, is beyond the scope of, and the available space for, the present paper.

29.3.4 Seasonal Variability

An important property of long-term *Es* variability is a well-defined annual *Es* dependence which is marked by a pronounced summer maximum. There exist several statistical studies (e.g., see Whitehead, 1989) which show that *Es* occurrence and intensity is marked by a conspicuous maximum which forms during June–July and December–January for the northern and southern hemispheres respectively, that is, around the northern and southern hemisphere summer solstices. This seasonal *Es* morphology is inexplicable from the windshear theory and constitutes for it an important weakness. Although there might be some seasonal differences in the tidal modes involved in *Es* formation, there exists no evidence to suggest that something dramatic is happening in the driving tides during summer which can account for the conspicuous summer maximum in occurrence and intensity. The annual *Es* dependence attracted considerable attention through the many years of *Es* research but, despite the efforts, no comprehensive explanation emerged until recently, when long term measurements of the meteoric, and thus metallic material, deposition in the atmosphere became available.

The role of metallic ions is recognized as an essential constituent in layer forming, and often it has been invoked as one of the reasons contributing to the sporadic nature of the phenomenon. Therefore, among the possibilities proposed for the explanation of *Es* summer maximum was also the increase of metal ion content (Whitehead, 1989). This was logical to consider since sporadic *E* is due to metallic ions provided by the atmospheric ablation of meteoroids, therefore the layer mean electron density (intensity) and occurrence are expected to depend directly on metallic material deposition in the lower thermosphere. The metallic ion variability as the cause for the *Es* summer maximum has been excluded however in earlier studies on the basis that the meteoric influx was sporadic and that no evidence existed in favour of a strong seasonal dependence.

The option of metallic ion seasonal dependence and its effect on sporadic *E* occurrence and intensity was brought up again recently after the publication of a series of meteor radar measurements in both the northern and southern hemispheres. These studies revealed a strong seasonal dependence for the daily meteor count rates which, as in sporadic *E*, it was marked by a pronounced summer maximum (e.g., see Singer et al., 2004; Janches et al., 2004; Lau et al., 2006). This variability was attributed to the fact that the sporadic meteor radiants are not randomly distributed in the sky but arrive from well-defined sources located near the ecliptic plane.

By using some of these meteor measurements, a recent study by Haldoupis et al. (2007) established a close correlation between the annual variation of ionosonde sporadic *E* layer intensities and meteoric deposition rates. Figure 29.8, illustrates the good correlation that exists between the mean annual variation of daily meteor counts measured in northern Europe over a period of 6 years, and simultaneous *foEs* daily means taken from an ionosonde station in the European midlatitude sector. The quantity *foEs* is the layer critical ionosonde frequency which relates approximately to the maximum electron density N_{em} through $foEs = 9.0\ (N_{em})^{1/2}$ (where N_{em} is measured in m^{-3} and *foEs* in Hz). Since the occurrence and strength of sporadic *E* layers depends directly on the metal ion content, which apparently is determined by meteoric deposition, the findings of Haldoupis et al. (2007) offered for the first time a likely cause-and-effect explanation for the long-going mystery of sporadic *E* layer

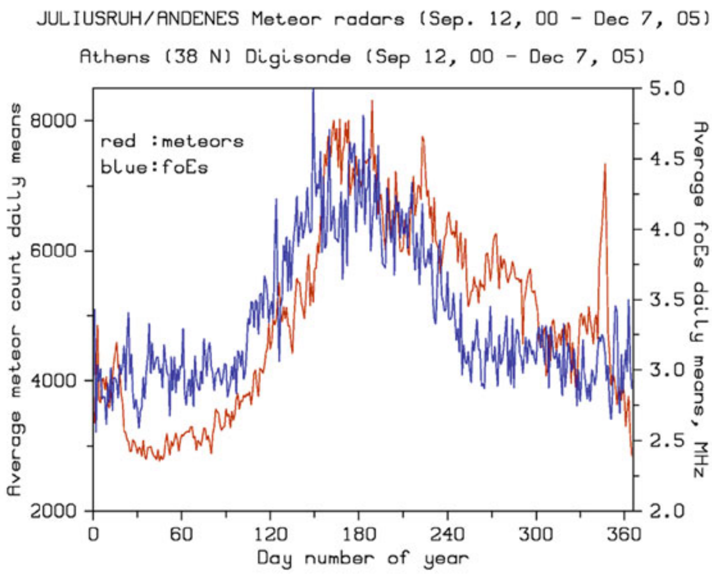

Fig. 29.8 Comparison of the mean annual variation of daily mean meteor counts measured partly in Juliusruh and partly in Andenes (*red line*), and ionosonde *foEs* statistics measured by the Athens ionosonde (38.0°N) for the period from September 2000 to December 2005. As seen, the correlation between meteor count rates and sporadic *E* intensity is fairly good, suggesting a cause and effect relationship

seasonal dependence. This agrees well with the established importance of metallic ions in the formation of sporadic E.

29.3.5 Global Es Occurrence and Variability

There are several studies on the world-wide distribution of Sporadic *E* made in the 70's and 80's, which were based on routine ionosonde observations from as many locations as possible (see Whitehead, 1989 for a discussion and references). Although most of these studies agreed that the strongest and most frequent layers occur at midlatitudes, their findings differed widely, a fact that might have been anticipated, given the few reliable ionosondes that were available at that time plus their uneven global distribution. Several of the early studies suggested as a reason for the world-wide occurrence and intensity of *Es* the global variability of the horizontal magnetic field component, *H*, whereas others found a small *H* dependence, or attributed the *Es* global distribution to the world-wide thunderstorm activity. Also there have been findings which contradicted the wind shear theory, for example reports on strong blanketing sporadic *E* layers near the magnetic equator where layer formation is, according to theory, inhibited. Although there are valuable information in all these old studies, which are characterized by great scientific intuition and thoroughness, overall they have been inconclusive and failed to provide an acceptable picture on the global distribution of sporadic *E* and the physical reasons behind it.

The answer to the problem of *Es* global distribution came only recently with the use of a new methodology which involved LEO (low earth orbiting) satellite GPS (global positioning system) occultation measurements that have the advantage of good global coverage (e.g., see Hocke and Tsuda, 2001). The GPS signals received at LEO satellites are modified by refractive index changes in the atmosphere and ionosphere and their analysis can provide information on various atmospheric parameters including electron density fluctuations. The method has been particularly suitable for observing GPS signal occultations caused by electron density perturbations in relation with sporadic *E* layers. The analysis of LEO occultation data yields information on the occurrence of sporadic *E* with good spatial (geographic) and altitude resolution. Thus, the method has been used for measuring the distribution of sporadic *E* world-wide (e.g., Hocke et al., 1981; Wu et al., 2005; Wu, 2006; Arras et al., 2008)

The most complete study to date on the global distribution of Sporadic *E* occurrence, which is based on a large data base of GPS radio occultations obtained with LEO satellites, was made by Arras et al. (2008). Figure 29.9 (courtesy of *Christina Arras*) shows the global distribution of sporadic *E* during all 4 seasons,

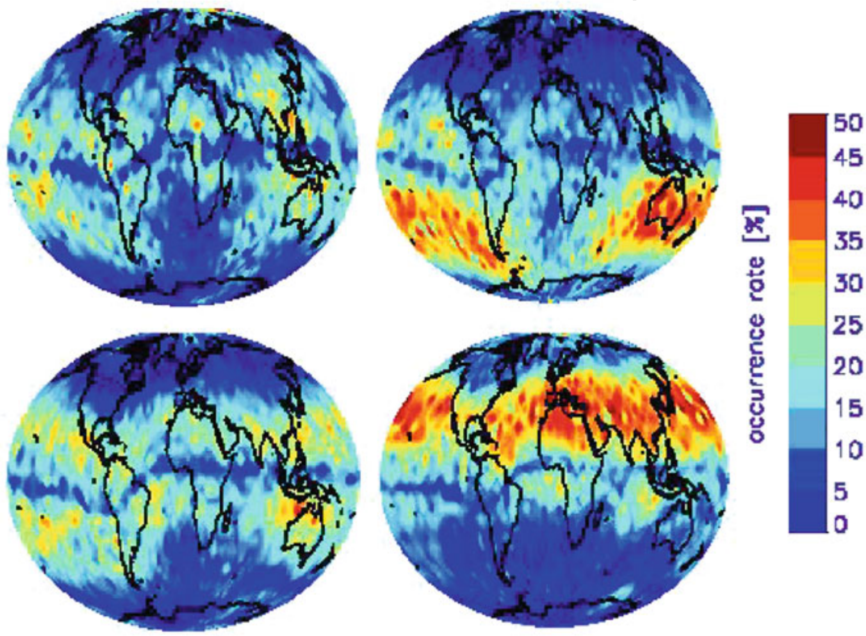

Fig. 29.9 Global distribution of sporadic *E* layer occurrence during the (north hemisphere) four seasons of 1 year (2006–2007): fall (*top left*), winter (*top right*), spring (*bottom left*) and summer (*bottom right*), as measured by GPS radio occultation methods. See more text for details. (Figure is published in Arras et al. (2008) and is kindly provided by Christina Arras)

based on a single year of occultation data from three different LEO satellites, taken between September 2006 and August 2007. As seen, the world-wide distribution characteristics of sporadic *E* occurrence have been depicted quite clearly for all four seasons. The strong seasonal variability agrees very much with that discussed in the previous section, that is, sporadic *E* exhibits a pronounced summer maximum (right panels in Fig. 29.9).

As noted by Arras et al. (2008), Fig. 29.9 shows considerable structure in the global distribution of *Es* occurrence characterized by well-defined regions of maxima and minima. The maxima appear at the midlatitude zones between about 10 and 60 degrees geomagnetic latitude. Also seen is a striking reduction in *Es* occurrence inside a narrow zone of about 3–5 degrees in latitude centred at the magnetic equator, which prevails clearly during all seasons. This is in good agreement with the windshear theory which inhibits layer formation at small dip angles because of the unique magnetic filed geometry at the equator and the need for the plasma to remain neutral, as discussed before in the theoretical part of this paper. Also there are deep minima located at high latitudes where dip angles are larger than 70 to 80 degrees, which again agrees with the windshear theory, as discussed earlier in 2.1. Also, as pointed by Arras et al. (2008), *Es* occurrence increases at midlatitudes during summer solstices with two noticeable exceptions, that is, two deep minima: one over the south Atlantic anomaly in the southern hemisphere and the other over northern America in the northern hemisphere, that is, at the two midlatitude regions of the globe where the horizontal magnetic field, *H*, is strongly reduced. This points to a decisive role of *H* in *Es* formation through the Lorentz force that drives the ion-convergence in the zonal windshear mechanism.

To strengthen the importance of this last finding, Fig. 29.10 is provided that shows the global distribution of the horizontal magnetic field intensity *H,* computed from IGRF (international geomagnetic reference field) at 105 km altitude. A qualitative comparison of Figs. 29.9 and 29.10 shows that the horizontal magnetic field is the main reason behind the world-wide distribution of sporadic *E* occurrence at midlatitude, a result that is in good agreement with windshear theory. Since *H* is entering only in the zonal windshear mechanism, the evidence here favors the zonal windshear process as the main player in *Es* forming relative to the meridional windshear. This is logical to expect because the zonal windshear mechanism operates more effectively at lower *E* region heights where most of sporadic *E* layers are known to be situated.

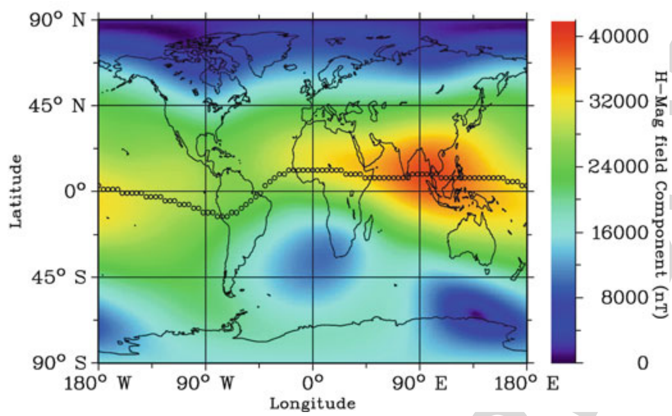

Fig. 29.10 Global map of the horizontal magnetic field component *H,* computed from the international geomagnetic reference (magnetic) field (IGRF) model. Comparison with Fig. 29.9, shows that the horizontal magnetic field component *H* is the key agent responsible for the global sporadic *E* occurrence distribution. This supports the windshear theory and the dominant role played in *Es* formation by the vertical shears in the horizontal zonal wind

29.4 Summary and Concluding Comments

The present paper is a tutorial review that provides a comprehensive update of our present basic knowledge on, and physical understanding of, midlatitude sporadic *E* layers (*Es*). It starts with a description of the *Es* windshear theory basics placing the emphasis on the physical picture defined by the driving forces and ion-convergence mechanisms of layer forming at different *E* region altitudes. Next, key observations are selected which are presented and discussed, showing that sporadic *E* layer formation and altitude descent are controlled by the vertical wind shears of atmospheric waves in the lower thermosphere. Although there is a number of parameters involved in sporadic *E* layer occurrence and intensity, which all may affect the overall *Es* formation and dynamics, the effects of the diurnal and semidiurnal tides though their vertical wind shears, remain prominent and are of fundamental importance.

Provided there is an abundance of metallic ions and atoms in the lower thermosphere, the close dependence of sporadic *E* on tidal wind shears, as the Arecibo incoherent scatter radar confirms, show that *Es* is a variable but a non-sporadic phenomenon. The present review places an emphasis on the “non-sporadic” character of sporadic *E* in order to draw attention to a fact that has so far been overlooked. That is, the non-sporadic character of *Es* is important because it implies that the physics of *Es* can be integrated in the existing atmosphere-ionosphere coupling models. In addition, the present paper discusses recent observations which provided long-waited explanations to problems associated with the seasonal dependence and global distribution of sporadic *E* layers. These findings identified the decisive contributions in sporadic *E* occurrence and intensity of the prominent seasonal dependence of meteoric deposition, and the global variability in the Earth’s horizontal magnetic field component. These, along with the diurnal and semidiurnal tides, are the key agents that control the variability and dynamics of sporadic *E.*

The present paper is far from a complete review of a rather diversified and long-studied subject. A complete treatise of sporadic E would have required dealing with additional *Es*-related processes and properties. Other than a brief reference to additional phenomena, the present paper does not deal with: (1) short term and/or quasi-periodic variations in sporadic *E* caused, possibly and partly, by gravity waves, and wind shear Kelvin-Helmholtz type instabilities, (2) short- and medium-scale electrostatic irregularities and plasma instabilities, and (3) electrodynamics and sporadic *E* – spread *F* coupling processes. All these are important topics of active and undergoing research. Also, other than a brief mention, the present paper did not deal with long-term variability in *Es* caused by planetary waves. The latter, which is a relatively new topic, is hoped to be dealt with in a separate publication.

Acknowledgements I wish to thank Dora Pancheva, Chris Meek, Sergei Shalimov, Qihou Zhou, Nikos Christakis, Alain Bourdillon, and Glenn Hussey, with whom I worked jointly the last several years in researching midlatitude sporadic *E* layers. Also wish to express my gratitude to Christina Arras for kindly providing Fig. 29.9 of this chapter. ELKE, University of Crete provided support for this work through grant 2746.

References

Arras C, Wickert J, Beyerle G, Heise S, Schmidt T, Jacobi C (2008) A global climatology of ionospheric irregularities derived from GPS radio occultation. Geophys Res Lett 35:L14809. doi:10.1029/2008GL034158

Axford WI (1963) The formation and vertical movement of dense ionized layers in the ionosphere. J Geophys Res 68:769

Bishop RL, Earle GD (2003) Metallic ion transport associated with midlatitude intermediate layer development. J Geophys Res 108:1019

Chapman S, Lindzen RS (1970) Atmospheric tides. D. Reidel, Hingham, MA

Chimonas G, Axford WI (1968) Vertical movement of temperate zone sporadic *E* layer. J Geophys Res 73:111

Christakis N, Haldoupis C, Zhou Q, Meek C (2009) Seasonal variability and descent of mid-latitude sporadic E layers at Arecibo. Ann Geophys 27:923–931

Djuth FT, Sulzer MP, Gonzales SA, Mathews JD, Elder JH (2004) A continuum of gravity waves in the Arecibo thermosphere. Geophys Res Let 31:L16801. doi:10.1029/2003GL019376

Forbes JM, Zhang X, Palo S, Russell J, Mertens CJ, Mlynczak M (2008) Tidal variability in the ionospheric dynamo region. J Geophys Res 113:A02310. doi:10.1929/2007JA012737

Haldoupis C, Meek C, Christakis N, Pancheva D, Bourdillon A (2006) Ionogram height-time intensity observations of descending sporadic *E* layers at mid-latitude. J Atmos Solar-Terr Phys 68:539

Haldoupis C, Pancheva D (2002) Planetary waves and midlatitude sporadic *E* layers: strong experimental evidence for a close relationship. J Geophys Res 107. doi:10.1029/2001JA000212

Haldoupis C, Pancheva D (2006) Terdiurnal tidelike variability in sporadic *E* layers. J Geophys Res 111:A07303. doi:10.1029/2005JA011522

Haldoupis C, Pancheva D, Mitchell NJ (2004) A study of tidal and planetary wave periodicities present in midlatitude sporadic E layers. J Geophys Res 109:A02302. doi:10.1029/2003JA010253

Haldoupis C, Pancheva D, Singer W, Meek C, MacDougall J (2007) An explanation for the seasonal dependence of midlatitude sporadic *E* layers. J Geophys Res 112:A06315. doi:10.1029/2007JA012322

Harper RM (1997) Tidal winds in the 100- to 200-km region at Arecibo. J Geophys Res 82:3243

Hocke K, Tsuda T (2001) Gravity waves and ionospheric irregularities over tropical convection zones observed by GPS/MET radio occultation. Geophys Res Lett 28: 2815–2818

Hocke K, Igarashi K, Nakamura M, Wilkinson P, Wu J, Pavelyev A, Wickert J (2001) Global sounding of sporadic E layers by the GPS/MET radio occultation experiment. J Atmos Solar-Terr Phys 63:1973–1980

Hysell DL, Yamamoto M, Fukao S (2000) Imaging radar observations and theory of type I and type II quasiperiodic echoes. J Geophys Res 107:1360

Janches D, Palo SE, Lau EM, Avery SK, Avery JP, de la Pena S, Makarov NA (2004) Diurnal and seasonal variability of the meteoric flux at the South Pole measured with radars. Geophys Res Lett 31:L20807. doi:10.1029/2004GL021104

Kelley MC (2009) The earth's ionosphere: plasma physics and electrodynamics, 2nd edn. Academic, San Diego, CA, p 281

Larsen MF (2000) A shear instability seeding mechanism for quasiperiodic echoes. J Geophys Res 105(24):931

Larsen MF (2002) Winds and shears in the mesosphere and lower thermosphere: Results from four decades of chemical release wind measurements. Geophys Res Lett 107:1215. doi:10.1029/2001JA000218

Larsen MF, Liu AZ, Gardner CS, Kelley MC, Collins S, Friedman J, Hecht JH (2004) Observations of overturning in the upper mesosphere and lower thermosphere. J Geophys Res 109:D02S04. doi:10.1029/2002JD003076

Lau EM, Avery SK, Avery JP, Janches D Palo SE, Schafer R, Makarov NA (2006) Statistical characterization of meteor trail distribution at the south pole as seen by a VHF interferometric meteor radar. Radio Sci 41:RS4007. doi:10.1029/2005RS003247

MacDougall JW, Plane JM, Jayachandran PT (2000) Polar cap Sporadic E: part 2, modeling. J Atmos Solar-Terr Phys 62:1169–1176

Mathews JD (1998) Sporadic *E*: current views and recent progress. J Atmos Solar-Terr Phys 60:413

Pancheva D, Haldoupis C, Meek CE, Manson AH, Mitchell NJ (2003) Evidence of a role for modulated atmospheric tides in the dependence of sporadic *E* on planetary waves. J Geophys Res 108. doi:10.1029/2002JA009788

Singer W, von Zahn U, Weiss J (2004) Diurnal and annual variations of meteor rates at the arctic circle. Atmos Chem Phys 4:1355–1363

Whitehead JD (1961) The formation of the sporadic E layer in the temperate zones. J Atmos Solar-Terr Phys 20:49

Whitehead JD (1989) Recent work on midlatitude and equatorial sporadic E. J Atmos Solar-Terr Phys 51:401

Wu DL (2006) Small-scale fluctuations and scintillations in high-resolution GPS/CHAMP SNR and phase data. J Atmos Solar-Terr Phys 68:999–1017

Wu DL, Ao CO, Hajj GA, de la Torre Juarez M, Mannucci J (2005) Sporadic E morphology from GPS-CHAMP radio occultation. J Geophys Res 110:A01306. doi:10.1029/2004JA010701